Published in final edited form as:
J Immunol. 2010 April 1; 184(7): 3598–3608. doi:10.4049/jimmunol.0902285.

Anergic CD4+ T cells form mature immunological synapses with enhanced accumulation of c-Cbl and Cbl-b[1]

Melissa Doherty[*,†], **Douglas G. Osborne**[*], **Diana L. Browning**[†], **David C. Parker**[‡], and **Scott A. Wetzel**[*,†]

[*]Division of Biological Sciences, The University of Montana, Missoula, MT. 59812

[†]Center for Environmental Health Sciences, The University of Montana, Missoula, MT. 59812

[‡]Department of Molecule Microbiology and Immunology, Oregon Health & Science, University, Portland, OR 97239

Abstract

CD4$^+$ T cell recognition of MHC:peptide complexes in the context of a costimulatory signal results in the large-scale redistribution of molecules at the T-APC interface to form the immunological synapse. The immunological synapse is the location of sustained TCR signaling and delivery of a subset of effector functions. T cells activated in the absence of costimulation are rendered anergic and are hyporesponsive when presented with antigen in the presence of optimal costimulation. Several previous studies have looked at aspects of immunological synapses formed by anergic T cells, but it remains unclear whether there are differences in the formation or composition of anergic immunological synapses. In this study we anergized primary murine CD4$^+$ T cells by incubation of costimulation-deficient, transfected fibroblast APC. Using a combination of TCR, MHC:peptide, and ICAM-1 staining, we found that anergic T cells make mature immunological synapses with characteristic cSMAC and pSMAC domains that were indistinguishable from control synapses. There were small increases in total phosphotyrosine at the anergic synapse along with significant decreases in phosphorylated ERK 1/2 accumulation. Most striking, there was specific accumulation of c-Cbl and Cbl-b to the anergic synapses. Cbl-b, previously shown to be essential in anergy induction, was found in both the pSMAC and the cSMAC of the anergic synapse. This Cbl-b (and c-Cbl) accumulation at the anergic synapse may play an important role in anergy maintenance and/or induction.

Introduction

Antigen recognition by CD4$^+$ T cells triggers the large-scale spatial redistribution of molecules to the T-APC interface to form a mature immunological synapse (1,2). The mature immunological synapse is characterized by the segregation of molecules into central and peripheral supramolecular activation clusters (cSMAC and pSMAC, respectively) (2). The prototypical mature immunological synapse has MHC:peptide, TCR and PKCθ accumulated in the cSMAC and molecules including ICAM-1 and LFA-1 accumulated in the pSMAC (1–3). Since its initial description more than a decade ago, there has been intense interest in the functions of this structure. The immunological synapse is the location of sustained signaling and TCR down-modulation (4–7). It also serves as the location of directional secretion for a subset of effector cytokines (8) and secretion of cytolytic granules by CD8$^+$ T cells (9). We,

[1]This work was supported by 2P20RR017670-06 Subproject 5 (S.A.W) and R01-AI-050823 (DCP).

Author for correspondence: Scott Wetzel, Division of Biological Sciences, 32 Campus Drive #4184, Missoula, MT 59812, Phone: (406) 243-2168, Fax: (406)243-4304, scott.wetzel@umontana.edu.

and others, have shown that costimulation enhances the formation of the mature immunological synapse (10–12).

In the absence of costimulation, T cells are rendered anergic (13,14), a hyporesponsive state characterized by alterations in intracellular signaling and establishment of an "anergy program" at the transcriptional level (14–18). One of the molecules expressed at significantly higher levels in anergic T cells is the E3 ubiquitin ligase Cbl-b (19–21). Cbl-b has been implicated in controlling the establishment and/or maintenance of the anergic phenotype (16,20,22). Cbl-b is expressed predominantly in mature peripheral T cells and is a negative regulator of TCR signaling (23). The closely related c-Cbl is found predominantly in thymocytes (24) and functions in the regulation of positive selection (25). Cbl-b is activated upon phosphorylation and functions, in part, by mediating TCR down-modulation (24,26–29), ubiquitin-mediated degradation of signaling molecules (19) and by altering the phosphorylation of Vav1(17,23, 30). Cbl-b$^{-/-}$ animals develop systemic autoimmunity (20,24,30,31), and T cells isolated from these animals display a hyperproliferative phenotype (23,30). Importantly, several studies have shown that Cbl-b$^{-/-}$ T cells are resistant to anergy induction (19,20,31), although evidence to the contrary has been recently published (32). Several studies have shown that Cbl-b is important in setting the requirement for CD28 costimulation of mature T cell activation (23, 33,34). A signal through CD28 in the context of TCR signaling leads to the ubiquitination and degradation of Cbl-b (17,21,33), while a signal through CTLA-4 induces Cbl-b expression (21).

Our previous work, as well as that of several other groups, has demonstrated that differences in the developmental or differentiation state of T cells are reflective of differences in the morphology and/or molecular accumulation/segregation at the immunological synapse (35–37). Because the anergic phenotype includes alterations in intracellular signaling, the transcriptional program and effector functions, we hypothesized that the immunological synapses formed by anergic T cells would be significantly different than control synapses. Several previous studies have examined aspects of the anergic immunological synapse (19, 38–41) and have shown that there is reduced recruitment of LAT (41) and lipid rafts, as shown by Cholera toxin B staining (39), and on anergic CD8$^+$ T cells, reduced CD45, Lck and CD8 accumulation (40). However, only two studies have examined the spatial distribution of molecules at the anergic synapse, and their results are contradictory. Carlin *et al.* (38) found CD3 distributed in arc/ring structure at the interface while Heissmeyer *et al.* found normal MHC:peptide recruitment to the mature anergic synapse at early time points (<22 min) (19). However, Heissmeyer *et al.* did report breakdown of the pSMAC ring at time points longer than 22 minutes (19). Clearly, much remains unknown about the immunological synapses formed by anergic T cells.

In this report we have examined the immunological synapses formed by anergic CD4$^+$ T cells and compared their morphology and molecular constituents to that of normal, rested T cell blasts. We show that anergic T cells form mature immunological synapses with the characteristic cSMAC and pSMAC domains. The amount and spatial distribution of accumulated MHC:peptide complexes at the anergic synapse does not differ significantly from that of the control synapse. However, when examining TCR signaling-associated molecules, we saw a slight increase in phosphorylated tyrosine and a significant reduction in phosphorylated ERK in the anergic synapse. F-Actin accumulation was slightly reduced, but the spatial distribution was indistinguishable from controls. Most significantly, we observed enhanced Cbl-b and c-Cbl recruitment to the T-APC interface. While these known negative regulators of TCR signaling were enhanced in the pSMAC of both control and anergic cells, the accumulation was significantly higher for the anergic cells. There was also accumulation of Cbl-b to the cSMAC of the anergic, but not control T cells. Thus, anergic CD4$^+$ T cells do make mature immunological synapses, but with altered molecular constituents.

MATERIALS AND METHODS

Animals

Heterozygous AD10 TCR transgenic mice ($V\beta3^+$), specific for pigeon cytochrome C (PCC) fragment 88–104 (42) and reactive against moth cytochrome C (MCC) fragment 88–103 on a B10.BR ($H\text{-}2^k$) background were kindly provided by Steve Hedrick (UCSD, San Diego, CA) by way of Philippa Marrack (National Jewish Medical Center, Denver, CO). Homozygous 3.L2 TCR transgenic mice ($V\beta8.3^+$), specific for peptide 64–76 of murine hemoglobin d allele (Hb), were kindly provided by Paul Allen (Washington University, St. Louis, MO) (43). These mice were bred and maintained in specific pathogen-free conditions in the animal care facilities at The University of Montana and at Oregon Health & Science University. Mice were allowed food and water *ad libidum*. AD10 TCR transgenic T cells were identified by PCR.

Antibodies and Staining Reagents

The following antibodies were purchased from Santa Cruz Biologicals (Santa Cruz, CA.): goat polyclonal anti-c-Cbl (sc-170-G), rabbit polyclonal anti-c-Cbl (sc-170), mouse monoclonal anti-Cbl-b (G-1), goat polyclonal anti-LAT (sc-5321). Phalloidin AlexaFluor 594 and Vybrant DiI were purchased from Molecular Probes (Eugene, OR.). A monoclonal anti-phosphorylated ERK 1/2 (T202/Y204; 9106), rabbit polyclonal anti-Lck (2751) and rabbit polyclonal anti-PLCγ1 (sc-81) were purchased from Cell Signaling (Beverly, MA). The monoclonal anti-phosphotyrosine 4G10 was purchased from Upstate Biotechnology (Lake Placid, NY). The anti-ICAM-1 (3E2), anti-Vβ3 (KJ25), and anti-CD69 (H1.2F3) were purchased from BD Biosciences (San Jose, CA.).The anti-CD4 (RM4–5) was purchased from BioLegend (San Diego, CA.). A polyclonal rabbit antibody to GRAIL (44) was a kind gift of Dr. Garrison Fathman at Stanford University.

Peptides

$MCC_{88–103}$ and $Hb_{64–76}$ were purchased from New England Peptide (Gardiner, MA) and resuspended at 500μM in PBS. They were diluted in complete RPMI for use.

Antigen Presenting Cells

Transfected Ltk^- fibroblasts were used as antigen presenting cells to induce anergy and in subsequent imaging and flow cytometry experiments. MCC:GFP fibroblasts expressing GFP-tagged $I\text{-}E^k$ β chain with covalent antigenic moth cytochrome C peptide have been described previously (12). The LMCC cell line expressing an MCC:$I\text{-}E^k$ β chain covalent construct with 3 repeats of the DNA gyrB domain on the cytoplasmic tail have also been previously described (45). The levels of $I\text{-}E^k$:MCC on the LMCC and MCC:GFP cells are very similar, but LMCC cells express very low levels of CD80 and ICAM-1 (12,46). Cells were maintained in DMEM (Sigma, St. Louis, MO.) containing 10% FBS (Atlanta Biologicals, Atlanta, GA) and supplemented with 1 mM L-glutamine, sodium pyruvate (100 mg/ml), 50 μM 2-ME, essential and non-essential amino acids, 100 U/ml penicillin G, 100 U/ml streptomycin, and 50 μg/ml gentamycin (Sigma, St. Louis, MO.).

The $I\text{-}E^{k+}$ CH27 B cell lymphoblast cell line, a gift of Brian Evavold at Emory University, was used to present antigen in proliferation assays. These cells were maintained in RPMI 1640 (Sigma, St. Louis, MO.) containing 10% FBS (Atlanta Biologicals, Atlanta, GA) and supplemented with 1 mM L-glutamine, sodium pyruvate (100 mg/ml), 50 μM 2-ME, essential and non-essential amino acids, 100 U/ml penicillin G, 100 U/ml streptomycin, and 50 μg/ml gentamycin (Sigma, St. Louis, MO.).

$CD4^+$ T Cell Generation and Anergy Induction

AD10 spleens were harvested and single cell suspensions were prepared by gentle grinding between sterile ground glass slides. After hypotonic lysis of red blood cells, lymphocytes were enriched by density centrifugation using Lympholyte M (Cedarlane, Burlington, NC). The lymphocyte-enriched cell suspension was resuspended at ~4×10^6/ml in complete RPMI and incubated for 4 days with 2.5μM MCC peptide. On day 2, RPMI-10 was added to the cultures to double the initial volume. No exogenous IL-2 was added during the culture period.

Anergy was induced using $CD80^{low}$ LMCC fibroblast APC as previously described (45). Briefly, day 4 T cell blasts cells were harvested from the *in vitro* culture and live cells were enriched by density centrifugation on Lympholyte M. 5×10^6/ml cells were added to a 100 mm Nuncalon Tissue culture treated Petri dish (Nunc, Rochester, N.Y.) containing 5×10^6 LMCC fibroblast APC. After a 24 hour incubation, T cells were recovered and cultured for an additional 4 – 6 days without antigen presenting cells or exogenous IL-2. Control T cells were recovered from the initial blast culture on the day of the experiment (9 to 11 days after initial culture was established).

Measurement of T cell Proliferation

Proliferation of the AD10 T cells in response to $MCC_{88–103}$ peptide-pulsed CH27 cells was measured by a standard 72-hour [^{3}H] thymidine incorporation assay. 2.5×10^4 control or anergized AD10 T cells were incubated with 5×10^4 mitomycin C-treated CH27 cells pulsed with varying amounts of $MCC_{88–103}$ peptide. Cultures were pulsed with 1 μ Ci [^{3}H] thymidine (2 Ci/mmol specific activity) during the last 12 hours of a 72 hour assay. Cells were harvested and radioactivity was measured using a Packard Top Count (Packard Instruments, Waltham, MA.).

T Cell Activation by Flow Cytometry

2.5×10^6 T cells and 1×10^6 MCC:GFP cells per well in a 6 well plate were incubated overnight (12 – 18 hours) in 3 ml total volume of complete RPMI. T cells were recovered from the wells and stained for CD4, Vβ3, and CD69 for 30 minutes at 4° in FACS buffer (PBS + 2% BSA Fraction V + 0.1% NaN_3). After 3 washes, cells were stained for 20 minutes with secondary reagents in FACS buffer. After 3 additional washes, cells were examined using a FACSAria (BD Biosciences, San Jose, CA) and data was analyzed using FlowJo 8 (Treestar, Inc, Ashland, OR).

Fixed Cell Microscopy

Imaging experiments were carried out in #1.5 LabTek II 8-chambered coverslips (Campbell, CA). One day before use, 2.5×10^4 MCC:GFP cells were added per well and incubated overnight at 37°. After addition of 10^5 T cells, dishes were spun briefly to initiate contact between T cells and APC and subsequently incubated for 30 minutes at 37°. Cells were fixed by addition of ice-cold fixative (4% paraformaldehyde, 0.5 % glutaraldehyde in PBS) and incubated for 45 minutes at room temperature in the dark followed by permeabilization with 0.2% Triton X-100 in PBS for 10 minutes. Cultures were stained with primary antibodies at 10 μg/ml in PBS for 2 hours at room temperature in a humidified chamber. Following 3 PBS washes, cells were incubated with secondary antibodies at 5 μg/ml, or phalloidin (1:500 dilution in PBS), for 2 hours at room temperature. After 3 additional PBS washes, SlowFade® Gold anti-fade reagent (Molecular Probes, Eugene, OR) was added to the wells. Samples were stored at 4° protected from light until imaged.

T Cell – APC conjugates to be imaged were chosen based upon their characteristic morphology in DIC of T cells in tight contact with, and flattened against, an APC. A stack of 50 – 90

fluorescent images spaced 0.2 μm apart in the *z*-axis was obtained with a 60×, 1.4 NA, oil immersion lens on the Applied Precision (API) DeltaVisionRT® image restoration microscopy system (Issaquah, WA). Deconvolution was performed using an iterative, constrained algorithm module in the Applied Precision SoftWorx software package. 3-Dimensional reconstructions and further image analysis was performed using the API SoftWorx software package. Co-localization was analyzed using ImageJ (47) and the JACoP plugin (48) to calculate the Pearson's correlation coefficient.

Live Cell Microscopy

For live cell microscopy, 2.5×10^4 APC were seeded into #1.5 LabTek II 8-chambered coverslips (Campbell, CA) 1 day prior to the experiment. Dishes were fitted onto the stage of the API DeltaVisionRT® image restoration system. Temperature was maintained at 37° for the duration of the imaging by the Weather Station® environmental chamber. After adding 1×10^5 AD10 T cells to a well, alternating green fluorescent (528 nm) and differential interference contrast (DIC) images were taken every 8 – 12 seconds for 60 minutes using a 60×, 1.4 NA lens. Image analysis was performed using the API SoftWorx software package along with ImageJ (47). Live cell experiments were performed in complete RPMI culture medium free of phenol red and bicarbonate.

Statistical Analysis and Graphing

Statistical analysis (ANOVA and student's t test) and graphing was performed using Prism 4 (GraphPad Software, La Jolla, CA.). Significance was defined as $p \leq 0.05$.

RESULTS

AD10 CD4$^+$ T cells are rendered anergic by 24 hour incubation on transfected fibroblast APC that express very low levels of CD80

The present study was designed to determine whether *in vitro* anergized CD4$^+$ T cells form mature immunological synapses and, if so, to characterize these synapses. Anergy was induced by a 24 hour incubation of day 4 T cell blasts on CD80^{low} LMCC fibroblast APC as previously described (45). To confirm anergy induction, the T cells were rested for 6 days after recovery from the co-culture with the LMCC cells before restimulation with CH27 B cells pulsed with $MCC_{88–103}$ antigenic peptide. As seen in Fig. 1A, the proliferative capacity of the T cells previously incubated with the LMCC fibroblast APC was significantly reduced compared to the control cells. Addition of 20U/ml of rmIL-2 during the 3 day proliferation assay rescued the proliferative capacity of the T cells pre-incubated on the LMCC cells. These results confirm that incubation with the LMCC fibroblast APC induces anergy in responding antigen-specific CD4$^+$ T cells.

The ability of the anergized CD4$^+$ T cells to respond to antigen was further characterized after overnight incubation on MCC:GFP fibroblasts (12). These cells express high levels of endogenous CD80 and have been transfected with ICAM-1, I-E^k α chain and a GFP-tagged I-E^k β chain with covalently attached $MCC_{88–103}$ antigenic peptide (12). To assess the antigen-responsiveness of the control and anergic T cells, we measured the surface expression of the TCR. Both control and anergized T cells clearly down-modulated their TCR after overnight stimulation by MCC:GFP cells (Fig. 1B), showing that both were antigen-responsive. Of note, the extent of TCR down modulation on stimulated cells was significantly higher for anergic T cells than for control T cells even though these cells had significantly reduced proliferation in response to antigen. The level of CD69 expression, an early activation marker, was increased on both control and anergic T cells after stimulation with the MCC:GFP cells (Fig. 1C). However, when compared to unstimulated T cells (filled histograms), the increase in CD69 expression on antigen-stimulated anergic cells was significantly less than that seen on the

control cells. The phenotype and proliferation of T cells anergized by 24 hour incubation on the LMCC fibroblasts is identical to T cells anergized by 24 hour incubation on anti-TCRβ coated plates (data not shown). Taken together, the results in Fig. 1 show that 24 hour co-culture with LMCC fibroblasts induces anergy in antigen-specific AD10 T Cell blasts. These anergized T cells remain antigen responsive, with the level of TCR down-modulation significantly greater and CD69 upregulation significantly lower than in control T cells following exposure to optimal stimulation.

Anergic T cells form stable T-APC conjugates at reduced frequency

The results in Fig. 1 show that $CD4^+$ AD10 T cells were rendered anergic by co-culture with the $CD80^{low}$ LMCC fibroblast APCs and retain the ability to interact with APC. Contact between $CD4^+$ T cells and APC initiates large-scale cytoskeletal and morphological changes within the T cells leading to conjugate formation and an increase in the T-APC contact area (49–51). The ability of anergized T cells to form stable conjugates with antigen presenting cells is unresolved. There have been studies showing no differences compared to control T cells (39,41) while others show significant reductions in conjugate formation by anergic T cells (38,40). The formation of T-APC conjugates is a prerequisite for the formation of mature immunological synapses, therefore it was essential to determine whether the *in vitro* anergized T cells formed stable conjugates with APC. DiI labeled T cells were mixed with MCC:GFP fibroblast APCs and conjugate formation was determined after 30 minutes by flow cytometry.

As seen in Fig. 2A, after a 30 minute incubation, control T cells form stable conjugates with the MCC:GFP fibroblast APC. The anergic T cells also form stable conjugates, but at a lower frequency than that seen with the control T cells (12.7 % vs. 7.27%, respectively). Although T-APC conjugate population formed by the anergic T cells was not as distinct as that of control cells, the frequency of anergic conjugates was still significantly higher than that seen with the non-specific $I\text{-}E^k$:$Hb_{64–76}$-reactive 3.L2 T cells (4.11%). While the percentage of conjugates varied slightly from experiment to experiment (control range was 6.17% to 16.4% and anergic range was 4.4% to 11.9%) the difference between the three groups was consistent within each experiment. The frequency of stable control T-APC conjugates was 69.3 ± 8.45% (mean ± SEM) higher than the frequency of stable anergic T cell conjugates and 188.8% ± 24.1% higher than for the non-specific 3.L2 T cells.

Kinetics of immunological synapse formation by anergic T cells are similar to control T cells

The data in Fig. 2A showed that both control and anergic T cells have the ability to form stable conjugates, albeit with different frequency. To determine whether anergic $CD4^+$ T cells have the ability to form mature immunological synapses, we assessed the redistribution of the GFP-tagged MHC:peptide complexes and monitored T cell morphology during T-APC interactions by live-cell microscopy. Using this system, we previously showed that interaction with antigen-specific T cells leads to large-scale T cell morphological changes and the formation of small MHC:peptide clusters that coalesce to form an immunological synapse (12). In live-cell imaging experiments, we have defined a “mature” immunological synapse as a GFP cluster at the interface of a T cell and APC that has reached maximal size and fluorescence intensity (12).

As seen in Fig. 2B, the interaction of both control and anergic T cells with the MCC:GFP APC results in tight adherence and flattening against the APC with a dramatic increase in the contact area over a period of several minutes. After observing at least 125 individual T-APC interactions for both control and anergic T cells over 5 separate experiments, we found the characteristic morphological changes occurring as a consequence of antigen recognition were indistinguishable between the control and anergic T cells.

We also examined the kinetics of immunological synapse formation for control and anergic T cells during the live cell experiments by calculating the time between the initial T cell contact with an APC and the formation of the mature immunological synapse. For the control cells, the mean time between contact and mature immunological synapse formation was 394 ± 55.9 seconds (mean ± SEM) with a range of 180 to 1159 seconds. For the anergic cells, the mean time between contact and mature IS formation was slightly longer at 434 ± 92 seconds with a range of 244 to 1447 seconds. As with the morphological data, there was no significant difference in the kinetics of mature immunological synapse formation between control and anergic T cells.

Anergic T cells form mature immunological synapses with prototypical cSMAC and pSMAC domains

To confirm that the structures observed by live-cell microscopy were indeed immunological synapses, we performed 3D microscopy using fixed and antibody stained T-APC conjugates. A representative set of images from at least 200 control and anergic synapses over 5 separate experiments is shown in Fig. 2C. These images show specific accumulation of both the GFP-tagged MHC:peptide and the TCR at the interface of the control T cells and the APC. The intensity of TCR staining at the interface of both control and anergic T cells was at least 3 fold above other areas on the same T cell. The TCR and GFP-tagged MHC:peptide co-localized at the T-APC interface as seen by the yellow region at the interface in the merged image. The second T cell attached to the left side of the APC forms a similar TCR-MHC co-localized region in a separate optical section (data not shown). As with the live cell data, from an edge-on view, the co-localization of TCR and GFP-tagged MHC:peptide at the interface of the anergic T cells and the control T cells was virtually indistinguishable (Fig. 2C).

To confirm the TCR-MHC:peptide co-localization and to examine the spatial distribution of the MHC and TCR molecules at the T-APC interface, we generated 3D rotations of the interface from the optical sectioning data. For both the control and anergic T cell interfaces, there was very clear co-localization of the MHC:peptide and the TCR at the T-APC interface (yellow regions in Fig. 2D). The Pearson's correlation coefficient for areas of TCR intensity 3 fold or more over background localizing with areas of MHC:GFP 2 fold or more than background was 0.87 for control cells and 0.92 for the anergic cells. Thus, there was significant co-localization of the TCR and MHC:peptide at the T-APC interface for both control and anergic T cells, and there were no significant differences between the two groups.

The TCR and MHC:peptide are both constituents of the c-SMAC in the mature immunological synapse (2). To confirm that the accumulated material at the T-APC was part of a traditional, spatially segregated mature immunological synapse, we next examined components of the p-SMAC, ICAM-1 and its ligand LFA-1. The images in Fig. 2E are representative of over 200 T-APC conjugates imaged for both control and anergic T cells over 5 separate experiments. For both control and anergic T cells, there was central accumulation of the GFP-tagged MHC:peptide with a ring of ICAM-1 at least 2 fold above background surrounding the central GFP spot. Similar distributions were observed with LFA-1 staining (data not shown). This arrangement is characteristic of the cSMAC, pSMAC spatial distribution seen in mature immunological synapses (1,2).

Taken together, the data from Fig. 2 shows that anergic T cells can form stable conjugates with APC, and upon the interaction with APC, there is redistribution of specific MHC:peptide complexes to the T-APC interface with similar kinetics to control T cells. Further, this interaction leads to spatial segregation of TCR and MHC:peptide to a central region at the interface (the cSMAC) surrounded by a ring of ICAM-1 (the pSMAC). These are prototypical features of mature immunological synapses and their appearance at the anergic T cell – APC

interface strongly supports the idea that anergic T cells are capable of forming mature immunological synapses.

Spatial distribution and the amount of accumulated MHC:peptide at the anergic immunological synapse is similar to controls

Having shown that anergic T cells form immunological synapses with the characteristic cSMAC and pSMAC molecular segregation patterns, we began characterizing the synapses further to determine if there were qualitative or quantitative differences in the accumulation and/or distribution of MHC:peptide complexes between anergic and control synapses.

To calculate the area of the T-APC interface with accumulated GFP-tagged MHC:peptide, we generated *en face* views of the 3D interface (Fig. 3A). The total surface area of the T-APC interface region with GFP fluorescence intensity at least 2 fold higher than the non-interface regions of the APC membrane was summed. The data in Fig. 3B is representative of 7 experiments performed with more than 500 control and anergic synapses imaged. For the control cells, the area of GFP ≥2 fold above background was 3.69 ± 0.35 μm^2 (mean ± SEM), while for the anergic cells it was 3.59 ± 0.38μm^2. The total area of the accumulated MHC:peptide was slightly larger for the control synapses, but this slight difference was not statistically significant.

We next calculated the total integrated intensity of the GFP spots ≥2 fold above background across the control and anergic T-APC interfaces. The integrated intensity is a relative measure of the intensity of the GFP and is reflective of the total amount of material accumulated at the interface. The integrated intensity of GFP-tagged MHC:peptide at the control interfaces ≥ 2 fold above background was 47572 ± 4573, while for the anergic synapses it was 41607± 3905 (Fig. 3C). This indicated that like the total area values, the amount of accumulated MHC:peptide at the T-APC interface was slightly higher for the control T cells, but the difference was not statistically significant.

During the analysis of the *en face* views of the 3D rotations for the area and integrated intensity calculations, we noted several different characteristic morphological patterns of the MHC:peptide distributions at the interface with the APC for both control and anergic T cells. We classified these into 5 categories of distribution: central spot, multi-focal center, multi-focal across the interface, edge of the interface, and no specific accumulation at the interface. Examples of the first four of these morphologies are shown in Fig. 3D. Calculated frequencies for each morphological pattern for 1 representative experiment of 7 is shown in Fig. 3E. For both control and anergic cells, the majority of material was accumulated in a central location (61.6% for control cells and 60.7% for anergic cells), although there are slightly more anergic synapses with central spots and slightly more control synapses with multi-focal center distribution. The frequency of the multi-focal across the interface morphological pattern was also slightly higher for the control cells (30.8% vs. 27.4% for anergic cells). The main difference between the control and anergic cells was in the percentage of interfaces without specific MHC:peptide accumulation. Out of 127 control interfaces examined in this experiment, there were none that lacked accumulation of the GFP-tagged MHC:peptide at the interface. In contrast, 7.6% of the 131 anergic interfaces imaged in this experiment lacked accumulation of the MHC:peptide at the interface. Taken together, the results in Fig. 3 show that there is specific accumulation of the GFP-tagged MHC:peptide complexes at the T-APC interface for both control and anergic T cells. The amount of material and the area of the interface that it occupies are slightly lower for the anergic cells, but the differences did not reach statistical significance. Additionally, the spatial distribution patterns of the accumulated MHC:peptide were similar for the control and anergic cells, although a small percentage of the anergic T cell – APC conjugates do not have accumulation of the MHC:peptide at the interface.

F-Actin accumulation at the anergic synapse is slightly reduced, but spatial distribution is not altered

The results in Fig. 2 and Fig. 3 suggest that anergic T cells were making relatively normal immunological synapses. However, the MHC:peptide distribution is only one aspect of the immunological synapse. To further characterize the immunological synapses formed by anergic T cells, we stained control and anergic T-APC conjugates for several other molecules.

Actin polarization and spatial re-distribution are critical for immunological synapse formation and formation of signaling microclusters (52–54). We began characterizing anergic synapse composition by looking at the total amount and spatial distribution of F-actin at the T-APC interface by staining with Phalloidin. The images in Fig. 4A clearly show that there was re-orientation of F-actin to the T-APC interface of both control and anergic T cells. When the control and anergic synapses were compared, there was a slight reduction in total F-actin accumulated at the anergic synapse. However, when viewed *en face*, the spatial distribution of the F-actin was indistinguishable from the control.

Phosphorylated tyrosine accumulation is slightly higher at anergic immunological synapse, while phosphorylated ERK 1/2 levels are significantly lower

We examined the spatial distribution of total phosphorylated tyrosine as a measure of TCR signaling at the immunological synapse. As shown Fig. 4B, there was appreciable accumulation of phosphorylated tyrosine (pTyr) to the interface of both control and anergic T cells. There was more pTyr at the anergic interface than at the control interface, although the difference in integrated intensity was not statistically significant (p=0.11) (Fig. 4B). The *en face* views showed areas of increased MHC:peptide intensity adjacent to areas of increase pTyr intensity at the center of the interface and their positions correlated very well. This correlation was found in more than 90% of both control and anergic T cells.

We also examined the level of phosphorylated ERK 1&2 accumulated at the T-APC interface in Figure 4C. Similar to the results in Figure 3, Figure 4A, and 4B, the amount of accumulated GFP-tagged MHC:peptide at the anergic immune synapse formed by the T cell on top of the APC is very similar to the accumulation at the control synapse. While there appear to be differences in the GFP accumulation between the two anergic T cells in Figure 4C, their accumulation is nearly identical. The two T cells form mature immune synapses in different focal planes and because the image in Figure 4C is a single optical section, it is not possible to display both synapses simultaneously. The control T cell images in Fig. 4C clearly show accumulation of pERK at the T-APC interface. This accumulation was more than 2 fold above background staining in 93% of the control immune synapses. For the controls, there was a slight reduction in the pERK intensity in the area where the clustered cSMAC MHC:peptide was accumulated, consistent with recent models suggesting the majority of signaling occurs in peripheral microclusters (6). By comparison, the accumulation of pERK at the anergic immunological synapse was significantly lower. The accumulated material only reached 1.25 to 1.5 fold above background in 79% of the anergic T-APC interfaces. Fewer than 5% of the anergic synapses had any areas that reached 2-fold above background, and where they occurred these areas were very small. This reduction in pERK accumulation is supported by the reduced CD69 upregulation observed in Fig. 1C and is consistent with Adams *et al.* (55).

Trogocytosis by anergic T cells

A very common feature of these fixed T-APC conjugate images was the transfer of small amounts of GFP-tagged MHC:peptide from the APC to the T cells. These small green spots were observed on the sides of the T cells in Fig. 4B (also visible in Fig. 2C). We saw this intercellular transfer, termed trogocytosis (56), on 85% of control conjugates and 82.4% of anergic conjugates. In the majority of these instances (52% for controls and 60.4% for anergic)

the transferred material had moved to the distal pole of the T cell, in an area directly opposite the interface. The significance of this intracellular molecular transfer is unclear. Interestingly, there was accumulation of pTyr to the spots transferred onto the T cells, suggesting sustained signaling at the location of the transferred MHC:peptide. This is in agreement with our previous data showing trogocytosed MHC:peptide in association with pTyr on the surface of T cells that spontaneously dissociated from APC (46).

At anergic immunological synapses c-Cbl and Cbl-b are enhanced in the pSMAC and Cbl-b is also accumulated in the cSMAC

The increase in total pTyr and reductions in pERK 1/2 and F-actin accumulation suggest that there are differences in the signaling from MHC:peptide-engaged TCR in the anergic cells. This is consistent with previous reports showing signaling defects in anergic T cells (14). Potential negative regulators of TCR signaling that have been implicated in altering TCR signaling in anergic T cells include the E3 ubiquitin ligases Cbl-b, c-Cbl and GRAIL (22). We examined the accumulation and spatial distribution of these molecules at the T-APC interface of control and anergic T cells. Our initial experiments found that GRAIL was not localized to the T-APC in either control or anergic T cells (data not shown) consistent with previous reports that have localized it to endocytic membranes (57). We did not characterize GRAIL distribution further.

There were significant differences between control and anergic T cells when the distribution of c-Cbl at the immunological synapse was compared. In the control T cells, the majority of cells (62.5%) had either no specific accumulation or exclusion from the T-APC interface region. This was slightly higher than what was found with the anergic T cells (54.5%). There was a small increase in c-Cbl 18.8% of the control T-APC interfaces, but this increase did not reach a threshold of 2 fold above background. By comparison, the proportion of anergic T cells with c-Cbl accumulation at the T-APC interface was similar to the controls (18.2%), but the intensity of staining was significantly higher (Fig. 5A). In all of the anergic T cell – APC interfaces examined, there was accumulation ≥ 2 fold above background staining levels, while none of the control synapses reached that threshold.

There were very clear differences in the spatial distribution of c-Cbl at the control and anergic T-APC interfaces when the *en face* views were compared (Figs. 5B and 5C). c-Cbl is distributed across the interface in a multi-focal pattern for 12.5% of the control synapses. This staining pattern was not observed with the anergic cells. For the majority of both control (64.8%) and anergic cells (83.4%) a ring of c-Cbl formed around the accumulated GFP-tagged MHC:peptide complexes. Interestingly, all of the anergic synapse c-Cbl rings reached ≥2 fold above background, but none of the control synapse c-Cbl rings reached that threshold. For the vast majority of both control and anergic synapses there was either no accumulation of c-Cbl at the center of the ring or the c-Cbl was excluded from the ring (Fig. 5C). However, a fraction (28%) of the anergic synapses with a c-Cbl ring ≥2 fold above background also had specific accumulation of c-Cbl in the center of the ring that reached a level ≥1.5 fold above background co-localized with MHC:peptide. This distribution pattern was not seen with the control cells. Thus, c-Cbl appears to be preferentially accumulated in the pSMAC of both control and anergic synapses, but there was significantly more c-Cbl in the anergic immunological synapses.

The accumulation of Cbl-b was significantly different between the anergic and control immunological synapses. Cbl-b levels were increased in virtually all control and anergic synapses (Fig. 5A) with the specific accumulation reaching a threshold of ≥2 fold above in 94.4% of the anergic synapses, while only 8.3% of the control synapses reached this threshold (Fig. 5D).

The spatial distribution of Cbl-b at the control and anergic synapses was also significantly different (Fig. 5E). For the control cells, 25.1% of the immunological synapses had uniform, dim (< 1.5 fold above background) Cbl-b staining across the interface while in the anergic synapses, this uniform staining was observed only 9.8% of the time (Fig. 5E). For the majority of control immunological synapses (74.9%), there was a dim ring of slightly enhanced Cbl-b staining (<2 fold above background) with either no enhanced central Cbl-b or exclusion of Cbl-b staining in the center of that ring (Fig. 5E). In 87% of these control synapses with a dim Cbl-b ring, the GFP-tagged MHC:peptide was found within the Cbl-b ring and there was no co-localization of these two molecules (Fig. 5B). As with c-Cbl, this distribution pattern was suggestive of a pSMAC localization for the Cbl-b in the control immunological synapses.

In contrast to the control immunological synapses, more than 94% of the anergic immunological synapses had an intense ring of Cbl-b staining ≥ 2 fold above background. Similar to the distribution of c-Cbl, this Cbl-b ring surrounds a central MHC:peptide region (Fig. 5B). In approximately two thirds of these anergic synapses with an intense Cbl-b ring (63.5%) there was also a dim central region of Cbl-b staining (1.25 – 1.5 fold above background) that co-localizes with the central MHC:peptide accumulation. For the remaining anergic interfaces (26.7%), there was an intense Cbl-b ring with enhanced Cbl-b staining (≥2 fold above background) in the center (Fig. 5E) that co-localizes with the accumulated central MHC:peptide (Fig. 5B).

The data in Fig. 5 clearly shows that both c-Cbl and Cbl-b are accumulated to the T-APC interface in the majority of both control and anergic synapses. However, the amount accumulated at the anergic synapses is significantly higher. Both c-Cbl and Cbl-b are localized in ring-like structures surrounding centrally accumulated MHC:peptide complexes, which strongly suggests that these negative regulators of TCR signaling are found in the pSMAC. In the vast majority of anergic synapses, there was also some Cbl-b, but not c-Cbl, accumulation in the c-SMAC that co-localized with the GFP-tagged MHC:peptide complexes, and by extension, the engaged TCR (Supplementary Movies 1 & 2, Fig. 5B).

Discussion

Antigen recognition by $CD4^+$ T cells in the absence of a costimulatory signal leads to the induction of anergy (13). Anergy is associated with alterations in intracellular signaling and resultant effector functions such as reductions of IL-2 and IFNγ secretion (14–16,58). The immunological synapse is important in sustained signaling (4) and delivery of a subset of effector cytokines (8) by $CD4^+$ T cells. In this report we have examined the immunological synapse formed by anergic T cells to determine whether alterations in anergized T cells are reflected in changes to the composition or structure of the immunological synapse.

The mature immunological synapse is characterized by a prototypical central supramolecular activation cluster (cSMAC) with accumulated MHC:peptide, TCR, and PKCθ, among others, surrounded by a peripheral SMAC (pSMAC) enriched in molecules such as LFA-1/ICAM-1 and talin (1–3). We found that anergic cells form mature immunological synapses with specific accumulation of GFP-tagged MHC:peptide complexes at the center of the T-APC interface (Fig. 2E, Fig. 3D and 3E). The amount of accumulated MHC:peptide, the area of the T-APC interface covered by the accumulated MHC:peptide, and the spatial distribution of these molecules did not differ significantly between the control and anergic synapses. In live cell imaging experiments, we found the kinetics of mature immunological synapse formation was similar for control and anergic T cells.

There is considerable debate in the literature as to the ability of anergic $CD4^+$ T cells to form mature immunological synapses. Our results would appear to be inconsistent with the findings

of Heissmeyer *et al.*, who showed in a planar lipid bilayer system that mature immunological synapses that formed by ionomycin-anergized $CD4^+$ T cells were not stable and were disintegrating at 1 hour (19). However, at shorter time points (≤ 22 minutes) anergic T cells formed mature synapses with an ICAM-1 ring surrounding accumulated central MHC:peptide (19) which is consistent with our findings. The possible instability of anergic synapses in our system may be reflected in lower frequencies of T-APC conjugates (Fig. 2A). Ise *et al.* also found significant reductions in TCR, PKCθ and cholera toxin B accumulation at the anergic T-APC interface (39). In contrast, Zambricki *et al.* found that there were no significant differences in the accumulation of LFA-1 (a pSMAC marker) or PKCθ (a cSMAC marker) between anergic and control synapses after 18 hours of T-APC co-culture (40). Neither Zambricki *et al.* or Ise *et al.* examined the spatial distribution of molecules at the immunological synapse as we have done in this report. Our results would initially appear to be at odds with Carlin *et al.* who showed with anergized human T cell lines that CD3ε and TCRζ were accumulated at the anergic T-APC interface predominantly in arc or ring-like structures after 30 minutes of T and APC co-culture (38) rather than the predominantly central accumulation we observed. This apparent discrepancy is likely due to differences in the level of specific MHC:peptide on the surface of the APC, since they state that at higher antigen doses, anergic T cells showed a predominantly central accumulation of both CD3ε and TCRζ (38). Thus, our results are consistent with many of these earlier reports, even those that would initially seem to be at odds with our findings, and confirm that anergic $CD4^+$ T cells do form mature immunological synapses.

After confirming that anergic T cells form mature immunological synapses, we examined these structures to further characterize the accumulation and spatial distribution of additional molecules. We found slightly reduced levels of F-actin accumulated at the anergic immunological synapse, but the spatial distribution was normal. This is consistent with previous studies that showed sustained accumulation and the correct location of the actin cytoskeleton is essential for formation and maintenance of the mature immunological synapse (52).

When we looked at molecules associated with intracellular signaling, we observed a slight, but not significant, increase in total phosphotyrosine accumulated at the anergic synapse confirming that there was antigen recognition and TCR triggering in the anergic cells. In contrast, the level of phosphorylated ERK was significantly reduced at the anergic synapse. This potentially explains the reduced CD69 upregulation observed in anergic cells (Fig. 1) since CD69 expression is mediated by the ERK signaling pathway (59). Adams *et al.* previously reported that phosphorylated ERK was found at the plasma membrane of activated control T cells after antigen recognition, but remained cytoplasmic in anergic T cells. However, the low-resolution laser scanning cytometry technique they employed was not able to determine potential changes at the T-APC interface (55). Our results show for the first time that there is a significant reduction in phosphorylated ERK at the anergic immunological synapse.

One of the most intriguing observations we made was the enhanced accumulation of the E3 ubiquitin ligases c-Cbl and Cbl-b at the anergic synapses (Fig. 5). c-Cbl and Cbl-b are important negative regulators of TCR signaling (23,28) and previous studies have shown that Cbl-b is a key regulator of anergy (20). These molecules have been observed to accumulate in the region of triggered TCR on normal T cells (60,61), but no previous studies have shown the accumulation and spatial distribution of Cbl-b and c-Cbl at the anergic immunological synapse. Our results show for the first time that both c-Cbl and Cbl-b are preferentially accumulated in the pSMAC of immunological synapses formed by T cells (Fig. 5), but the level of accumulation is significantly higher for anergic cells. In addition, for a majority of anergic T cells, Cbl-b is also enhanced in the cSMAC while c-Cbl is found in the cSMAC in a minority of anergic immunological synapses. These molecules were not found at appreciable levels in

cSMAC of control synapses. These findings have significant implications in the initiation and/or maintenance of the anergic state.

Triggering of the TCR by cognate MHC:peptide complexes leads to the activation of the Src family kinase Lck, which in turn phosphorylates and activates Cbl molecules (27,62). This leads to the ubiquitination of components of the TCR complex (62). The TCR is down-modulated after triggering and trafficked to the lysosomes for degradation rather than being recycled to the plasma membrane (24,63). This differential trafficking is a Cbl-dependent process that has been proposed to attenuate TCR-mediated signaling (24,28,63,64). We observed increased TCR down-modulation of the TCR in anergic T cells (Fig. 1), which is consistent with previously observed increased in Cbl-b expression in anergic T cells (19,21, 41). The level of Cbl-b in the anergic cells used in this study are comparable to the levels of Cbl-b induced by the ionomycin induced anergic state as described by Heissmeyer *et al.* (19) (data not shown).

Cbl molecules are key regulators of anergy (20) and our results are the first to demonstrate the preferential accumulation of these molecules at the anergic immunological synapse. Wiedemann *et al.* have previously observed that Cbl-b, pTyr, and ubiquitin localized to antibody triggered TCR in human T cell clones (61) and Naramura *et al.* proposed that Cbl-b and c-Cbl would destabilize the immunological synapse and terminate signaling (24). c-Cbl has been shown to control LAT microcluster persistence (64) and PLCγ1 degradation (65), and Heissmeyer *et al.* showed that the degradation of PLCγ1 was mediated, at least in part, by Cbl-b resulting in the disintegration of the pSMAC at anergic synapses (19). We have not examined the stability of control or anergic immunological synapses here. However, our Cbl-b and c-Cbl data supports the previous reports focusing on the signaling and potential stability of the anergic immunological synapse. Combining our current observations with those previously published findings, we would like to propose a tentative model for the events occurring at the anergic immunological synapse. Antigen recognition by the anergic T cells combined with the activation of integrin “inside-out” signaling triggered by antigen recognition (66) leads to formation of a tight anergic T cell-APC conjugate. Over the next several minutes, small microclusters of MHC:peptide-engaged TCR form that coalesce into a mature immunological synapse with defined cSMAC and pSMAC domains. These microclusters in the nascent pSMAC have been shown to be the site of TCR signaling (6) and their persistence is controlled, in part, by c-Cbl-mediated ubiquitination (64). Cbl-b and c-Cbl are recruited to both the control and anergic immunological synapses, but at the control synapse CD28 signaling leads to the ubiquitination and destruction of the Cbl molecules as shown by Xhang *et al.* (21). With the lack of a CD28 signal during anergy induction Cbl molecules are not degraded leading to significantly higher expression of Cbl-b and c-Cbl in the anergic cells. At the subsequent immunological synapse formed by these anergic cells, our data here shows that Cbl-b and c-Cbl are preferentially accumulated compared to control T cells. At the anergic synapse they may mediate ubiquitination of several molecules, including the TCRζ, PLCγ1, and PI3K p85. At time points later than the 30 minutes used in this report, the Cbl-mediated ubiquitination may result in the destruction of PLCγ1 and hypophosphorylation of Vav1, altering the actin accumulation and distribution at the anergic synapse. The combination of actin disruption and cessation of PLCγ1-mediated signaling may result in immune synapse disintegration as the T cells re-initiate locomotion across the APC membrane as has previously been shown (19). Further experimentation will be necessary to confirm this model. Our finding that Cbl-b and c-Cbl preferentially accumulate at the anergic synapse and have altered spatial distribution provides critical information that aids in our understanding of the process of anergy maintenance in $CD4^+$ T cells.

Supplementary Material

Refer to Web version on PubMed Central for supplementary material.

Acknowledgments

The authors would like to thank the University of Montana Fluorescence Cytometry core and Pam Shaw for expert technical assistance with flow cytometry. We also thank Aurelie Snyder and the OHSU MMI Microscopy Core as well as the University of Montana Molecular Histology and Fluorescence Imaging core facility for technical assistance with imaging experiments. We also thank Dr. Yoshinobu Koguchi, Dr. Stephanie Lathrop, and Lindsay Thueson for critical review of the manuscript.

References

1. Grakoui A, Bromley SK, Sumen C, Davis MM, Shaw AS, Allen PM, Dustin ML. The immunological synapse: a molecular machine controlling T cell activation. Science 1999;285:221–227. [PubMed: 10398592]
2. Monks CR, Freiberg BA, Kupfer H, Sciaky N, Kupfer A. Three-dimensional segregation of supramolecular activation clusters in T cells. Nature 1998;395:82–86. [PubMed: 9738502]
3. Monks CRF, Kupfer H, Tamir A, Barlow A, Kupfer A. Selective modulation of protein kinase C-θ during T cell activation. Nature 1997;385:83–86. [PubMed: 8985252]
4. Huppa JB, Gleimer M, Sumen C, Davis MM. Continuous T cell receptor signaling required for synapse maintenance and full effector potential. Nat Immunol 2003;4:749–755. [PubMed: 12858171]
5. Lee KH, Dinner AR, Tu C, Campi G, Raychaudhuri S, Varma R, Sims TN, Burack WR, Wu H, Wang J, Kanagawa O, Markiewicz M, Allen PM, Dustin ML, Chakraborty AK, Shaw AS. The immunological synapse balances T cell receptor signaling and degradation. Science 2003;302:1218–1222. [PubMed: 14512504]
6. Varma R, Campi G, Yokosuka T, Saito T, Dustin ML. T cell receptor-proximal signals are sustained in peripheral microclusters and terminated in the central supramolecular activation cluster. Immunity 2006;25:117–127. [PubMed: 16860761]
7. Cemerski S, Das J, Giurisato E, Markiewicz MA, Allen PM, Chakraborty AK, Shaw AS. The balance between T cell receptor signaling and degradation at the center of the immunological synapse is determined by antigen quality. Immunity 2008;29:414–422. [PubMed: 18760640]
8. Huse M, Lillemeier BF, Kuhns MS, Chen DS, Davis MM. T cells use two directionally distinct pathways for cytokine secretion. Nat Immunol 2006;7:247–255. [PubMed: 16444260]
9. Stinchcombe JC, Bossi G, Booth S, Griffiths GM. The Immunological Synapse of CTL Contains a Secretory Domain and Membrane Bridges. Immunity 2001;15:751–761. [PubMed: 11728337]
10. Viola A, Schroeder S, Sakakibara Y, Lanzavecchia A. T lymphocyte costimulation mediated by reorganization of membrane microdomains. Science 1999;283:680–682. [PubMed: 9924026]
11. Wülfing C, Davis MM. A receptor/cytoskeletal movement triggered by costimulation during T cell activation. Science 1998;282:2266–2269. [PubMed: 9856952]
12. Wetzel SA, McKeithan TW, Parker DC. Live-cell dynamics and the role of costimulation in immunological synapse formation. J Immunol 2002;169:6092–6101. [PubMed: 12444111]
13. Jenkins MK, Pardoll DM, Mizuguchi J, Chused TM, Schwartz RH. Molecular events in the induction of a nonresponsive state in interleukin 2-producing helper T-lymphocyte clones. Proc Natl Acad Sci U S A 1987;84:5409–5413. [PubMed: 2955418]
14. Schwartz RH. T cell anergy. Annu Rev Immunol 2003;21:305–334. [PubMed: 12471050]
15. Wells AD. New insights into the molecular basis of T cell anergy: anergy factors, avoidance sensors, and epigenetic imprinting. J Immunol 2009;182:7331–7341. [PubMed: 19494254]
16. Fathman CG, Lineberry NB. Molecular mechanisms of $CD4^+$ T-cell anergy. Nat Rev Immunol 2007;7:599–609. [PubMed: 17612584]
17. Loeser S, Penninger JM. Regulation of peripheral T cell tolerance by the E3 ubiquitin ligase Cbl-b. Semin Immunol 2007;19:206–214. [PubMed: 17391982]

18. Macian F, Garcia-Cozar F, Im SH, Horton HF, Byrne MC, Rao A. Transcriptional mechanisms underlying lymphocyte tolerance. Cell 2002;109:719–731. [PubMed: 12086671]
19. Heissmeyer V, Macian F, Im SH, Varma R, Feske S, Venuprasad K, Gu H, Liu YC, Dustin ML, Rao A. Calcineurin imposes T cell unresponsiveness through targeted proteolysis of signaling proteins. Nat Immunol 2004;5:255–265. [PubMed: 14973438]
20. Jeon MS, Atfield A, Venuprasad K, Krawczyk C, Sarao R, Elly C, Yang C, Arya S, Bachmaier K, Su L, Brouchard D, Jones R, Gronski M, Ohashi PS, Wada T, Bloom D, Fathman CG, Liu YC, Penninger JM. Essential role of E3 ubiquitin ligase Cbl-b in T cell anergy induction. Immunity 2004;21:167–177. [PubMed: 15308098]
21. Li D, Gal I, Vermes C, Alegre ML, Chong AS, Chen L, Shao Q, Adarichev V, Xu X, Koreny T, Mikecz K, Finnegan A, Glant TT, Zhang J. Cutting edge: Cbl-b: one of the key molecules tuning CD28- and CTLA-4-mediated T cell costimulation. J Immunol 2004;173:7135–7139. [PubMed: 15585834]
22. Mueller DL. E3 ubiquitin ligases as T cell anergy factors. Nat Immunol 2004;5:883–890. [PubMed: 15334084]
23. Bachmaier K, Krawczyk C, Kozieradzki I, Kong YY, Sasaki T, Oliveira-dos-Santos A, Mariathasan S, Bouchard D, Wakeham A, Itie A, Le J, Ohashi PS, Sarosi I, Nishina H, Lipkowitz S, Penninger JM. Negative regulation of lymphocyte activation and autoimmunity by the molecular adaptor Cbl-b. Nature 2000;403:211–216. [PubMed: 10646608]
24. Naramura M, Jang IK, Kole H, Huang F, Haines D, Gu H. c-Cbl and Cbl-b regulate T cell responsiveness by promoting ligand-induced TCR down-modulation. Nat Immunol 2002;3:1192–1199. [PubMed: 12415267]
25. Naramura M, Kole HK, Hu RJ, Gu H. Altered thymic positive selection and intracellular signals in Cbl-deficient mice. Proc Natl Acad Sci U S A 1998;95:15547–15552. [PubMed: 9861006]
26. Elly C, Witte S, Zhang Z, Rosnet O, Lipkowitz S, Altman A, Liu YC. Tyrosine phosphorylation and complex formation of Cbl-b upon T cell receptor stimulation. Oncogene 1999;18:1147–1156. [PubMed: 10022120]
27. D'Oro U, Vacchio MS, Weissman AM, Ashwell JD. Activation of the Lck tyrosine kinase targets cell surface T cell antigen receptors for lysosomal degradation. Immunity 1997;7:619–628. [PubMed: 9390686]
28. Duan L, Reddi AL, Ghosh A, Dimri M, Band H. The Cbl Family and Other Ubiquitin Ligases: Destructive Forces in Control of Antigen Receptor Signaling. Immunity 2004;21:7–17. [PubMed: 15345216]
29. Shamim M, Nanjappa SG, Singh A, Plisch EH, LeBlanc SE, Walent J, Svaren J, Seroogy C, Suresh M. Cbl-b regulates antigen-induced TCR down-regulation and IFNγ production by effector CD8 T cells without affecting functional avidity. J Immunol 2007;179:7233–7243. [PubMed: 18025165]
30. Chiang YJ, Sommers CL, Jordan MS, Gu H, Samelson LE, Koretzky GA, Hodes RJ. Inactivation of c-Cbl reverses neonatal lethality and T cell developmental arrest of SLP-76-deficient mice. J Exp Med 2004;200:25–34. [PubMed: 15238603]
31. Wohlfert EA, Callahan MK, Clark RB. Resistance to $CD4^+CD25^+$ regulatory T cells and TGFβ in Cbl-$b^{-/-}$ mice. J Immunol 2004;173:1059–1065. [PubMed: 15240694]
32. St Rose MC, Qui HZ, Bandyopadhyay S, Mihalyo MA, Hagymasi AT, Clark RB, Adler AJ. The E3 ubiquitin ligase Cbl-b regulates expansion but not functional activity of self-reactive CD4 T cells. J Immunol 2009;183:4975–4983. [PubMed: 19801520]
33. Zhang J, Bardos T, Li D, Gal I, Vermes C, Xu J, Mikecz K, Finnegan A, Lipkowitz S, Glant TT. Cutting edge: regulation of T cell activation threshold by CD28 costimulation through targeting Cbl-b for ubiquitination. J Immunol 2002;169:2236–2240. [PubMed: 12193687]
34. Haglund K, Shimokawa N, Szymkiewicz I, Dikic I. Cbl-directed monoubiquitination of CIN85 is involved in regulation of ligand-induced degradation of EGF receptors. Proc Natl Acad Sci U S A 2002;99:12191–12196. [PubMed: 12218189]
35. Hailman E, Burack WR, Shaw AS, Dustin ML, Allen PM. Immature $CD4^+CD8^+$ thymocytes form a multifocal immunological synapse with sustained tyrosine phosphorylation. Immunity 2002;16:839–848. [PubMed: 12121665]

36. Lee SJ, Hori Y, Chakraborty AK. Low T cell receptor expression and thermal fluctuations contribute to formation of dynamic multifocal synapses in thymocytes. Proc Natl Acad Sci U S A 2003;100:4383–4388. [PubMed: 12671067]
37. Thauland TJ, Koguchi Y, Wetzel SA, Dustin ML, Parker DC. T_h1 and T_h2 cells form morphologically distinct immunological synapses. J Immunol 2008;181:393–399. [PubMed: 18566405]
38. Carlin LM, Yanagi K, Verhoef A, Nolte-'t Hoen EN, Yates J, Gardner L, Lamb J, Lombardi G, Dallman MJ, Davis DM. Secretion of IFNγ and not IL-2 by anergic human T cells correlates with assembly of an immature immune synapse. Blood 2005;106:3874–3879. [PubMed: 16099874]
39. Ise W, Nakamura K, Shimizu N, Goto H, Fujimoto K, Kaminogawa S, Hachimura S. Orally tolerized T cells can form conjugates with APCs but are defective in immunological synapse formation. J Immunol 2005;175:829–838. [PubMed: 16002680]
40. Zambricki E, Zal T, Yachi P, Shigeoka A, Sprent J, Gascoigne N, McKay D. *In vivo* anergized T cells form altered immunological synapses *in vitro*. Am J Transplant 2006;6:2572–2579. [PubMed: 16952297]
41. Hundt M, Tabata H, Jeon MS, Hayashi K, Tanaka Y, Krishna R, De Giorgio L, Liu YC, Fukata M, Altman A. Impaired activation and localization of LAT in anergic T cells as a consequence of a selective palmitoylation defect. Immunity 2006;24:513–522. [PubMed: 16713970]
42. Kaye J, Vasquez NJ, Hedrick SM. Involvement of the same region of the T cell antigen receptor in thymic selection and foreign peptide recognition. J Immunol 1992;148:3342–3353. [PubMed: 1316916]
43. Kersh GJ, Donermeyer DL, Frederick KE, White JM, Hsu BL, Allen PM. TCR transgenic mice in which usage of transgenic α- and β-chains is highly dependent on the level of selecting ligand. J Immunol 1998;161:585–593. [PubMed: 9670931]
44. MacKenzie DA, Schartner J, Lin J, Timmel A, Jennens-Clough M, Fathman CG, Seroogy CM. GRAIL is up-regulated in $CD4^+$ $CD25^+$ T regulatory cells and is sufficient for conversion of T cells to a regulatory phenotype. J Biol Chem 2007;282:9696–9702. [PubMed: 17259178]
45. Dillon TJ, Karpitski V, Wetzel SA, Parker DC, Shaw AS, Stork PJ. Ectopic B-Raf expression enhances extracellular signal-regulated kinase (ERK) signaling in T cells and prevents antigen-presenting cell-induced anergy. J Biol Chem 2003;278:35940–35949. [PubMed: 12855697]
46. Wetzel SA, McKeithan TW, Parker DC. Peptide-specific intercellular transfer of MHC class II to $CD4^+$ T cells directly from the immunological synapse upon cellular dissociation. J Immunol 2005;174:80–89. [PubMed: 15611230]
47. Rasband, WS. ImageJ. National Institues of Health; 1997–2009. http://rsb.info.nih.gov/ij/
48. Bolte S, Cordelieres FP. A guided tour into subcellular colocalization analysis in light microscopy. J Microsc 2006;224:213–232. [PubMed: 17210054]
49. Delon J, Bercovici N, Liblau R, Trautmann A. Imaging antigen recognition by naive $CD4^+$ T cells: compulsory cytoskeletal alterations for the triggering of an intracellular calcium response. Eur J Immunol 1998;28:716–729. [PubMed: 9521082]
50. Donnadieu E, Bismuth G, Trautmann A. Antigen recognition by helper T cells elicits a sequence of distinct changes of their shape and intracellular calcium. Curr Biol 1994;4:584–595. [PubMed: 7953532]
51. Negulescu PA, Krasieva TB, Khan A, Kerschbaum HH, Cahalan MD. Polarity of T cell shape, motility, and sensitivity to antigen. Immunity 1996;4:421–430. [PubMed: 8630728]
52. Tskvitaria-Fuller I, Rozelle AL, Yin HL, Wulfing C. Regulation of sustained actin dynamics by the TCR and costimulation as a mechanism of receptor localization. J Immunol 2003;171:2287–2295. [PubMed: 12928373]
53. Campi G, Varma R, Dustin ML. Actin and agonist MHC-peptide complex-dependent T cell receptor microclusters as scaffolds for signaling. J Exp Med 2005;202:1031–1036. [PubMed: 16216891]
54. Dustin ML. The cellular context of T cell signaling. Immunity 2009;30:482–492. [PubMed: 19371714]
55. Adams CL, Grierson AM, Mowat AM, Harnett MM, Garside P. Differences in the kinetics, amplitude, and localization of ERK activation in anergy and priming revealed at the level of individual primary T cells by laser scanning cytometry. J Immunol 2004;173:1579–1586. [PubMed: 15265885]

56. Joly E, Hudrisier D. What is trogocytosis and what is its purpose? Nat Immunol 2003;4:815. [PubMed: 12942076]
57. Anandasabapathy N, Ford GS, Bloom D, Holness C, Paragas V, Seroogy C, Skrenta H, Hollenhorst M, Fathman CG, Soares L. GRAIL: an E3 ubiquitin ligase that inhibits cytokine gene transcription is expressed in anergic $CD4^+$ T cells. Immunity 2003;18:535–547. [PubMed: 12705856]
58. Macián F, Im SH, García-Cózar FJ, Rao A. T-cell anergy. Curr Opin Immunol 2004;16:209–216. [PubMed: 15023415]
59. Denny MF, Kaufman HC, Chan AC, Straus DB. The Lck SH3 domain is required for activation of the mitogen-activated protein kinase pathway but not the initiation of T-cell antigen receptor signaling. J Biol Chem 1999;274:5146–5152. [PubMed: 9988764]
60. Eisenbraun MD, Tamir A, Miller RA. Altered Composition of the Immunological Synapse in an Anergic, Age- Dependent Memory T Cell Subset. J Immunol 2000;164:6105–6112. [PubMed: 10843659]
61. Wiedemann A, Muller S, Favier B, Penna D, Guiraud M, Delmas C, Champagne E, Valitutti S. T-cell activation is accompanied by an ubiquitination process occurring at the immunological synapse. Immunol Lett 2005;98:57–61. [PubMed: 15790509]
62. Cenciarelli C, Wilhelm KG Jr, Guo A, Weissman AM. T cell antigen receptor ubiquitination is a consequence of receptor-mediated tyrosine kinase activation. J Biol Chem 1996;271:8709–8713. [PubMed: 8621503]
63. Geisler C. TCR trafficking in resting and stimulated T cells. Crit Rev Immunol 2004;24:67–86. [PubMed: 14995914]
64. Balagopalan L, Barr VA, Sommers CL, Barda-Saad M, Goyal A, Isakowitz MS, Samelson LE. c-Cbl-mediated regulation of LAT-nucleated signaling complexes. Mol Cell Biol 2007;27:8622–8636. [PubMed: 17938199]
65. Rellahan BL, Graham LJ, Tysgankov AY, DeBell KE, Veri MC, Noviello C, Bonvini E. A dynamic constitutive and inducible binding of c-Cbl by PLCγ1 SH3 and SH2 domains (negatively) regulates antigen receptor-induced PLCγ1 activation in lymphocytes. Exp Cell Res 2003;289:184–194. [PubMed: 12941616]
66. Mor A, Dustin ML, Philips MR. Small GTPases and LFA-1 reciprocally modulate adhesion and signaling. Immunol Rev 2007;218:114–125. [PubMed: 17624948]

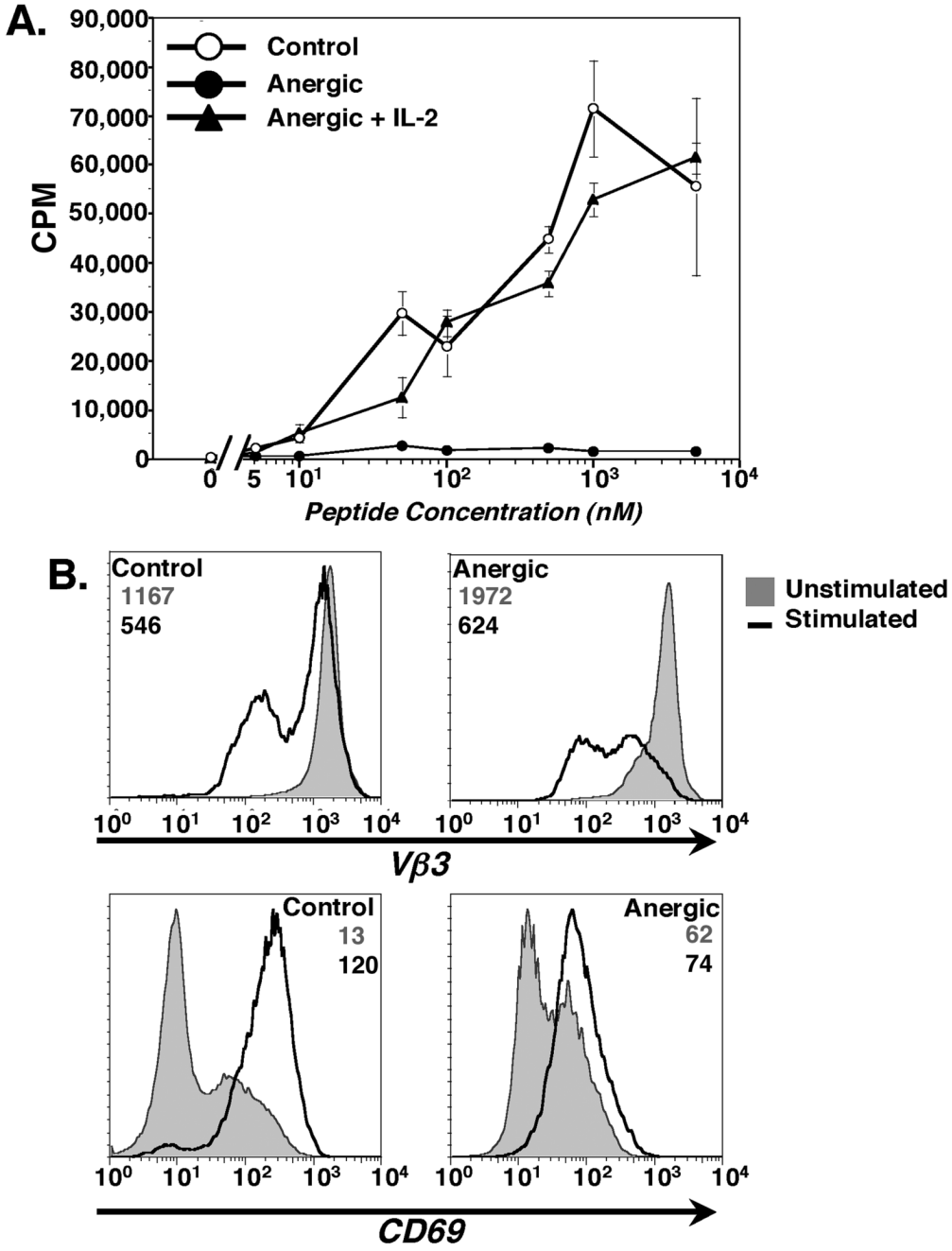

Figure 1. AD10 T cells stimulated by CD80^{low} LMCC transfected fibroblasts for 24 hours are rendered anergic

(A). Proliferation of control and anergized AD10 T cells measured by a standard ^{3}H-Thymidine incorporation assay. Cultures were pulsed with ^{3}H-Thymidine for the final 12 hours of a 72-hour assay. Addition of 20U/ml rmIL-2 restored proliferation to anergic cells. Values are mean CPM ± SEM. (B & C). TCR down-modulation (B) and CD69 upregulation (C) after overnight incubation of control or anergic T cells with MCC:GFP APC. Unstimulated cells(▬) and cells stimulated overnight on MCC:GFP cells (▩) are shown. Geometric mean fluorescence intensity values are indicated with gray representing unstimulated cells and black numbers APC-stimulated cells. Results are representative of 6 separate experiments.

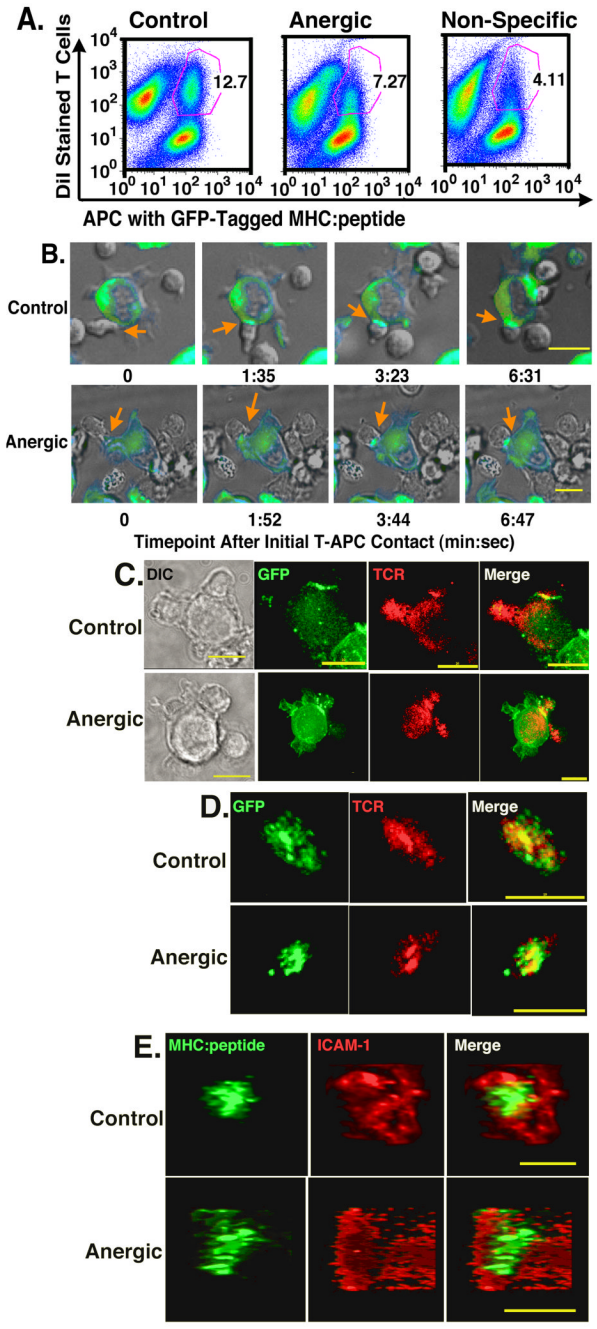

Figure 2. Anergized T cells have reduced efficiency of making T-APC conjugates, but form mature synapses with normal kinetics

(A) DiI stained control (left), anergic (center) or non-specific (right) T cells were incubated for 30 minutes with APC transfected with GFP-tagged MHC:peptide complexes. Conjugate formation was examined by flow cytometry. The numbers represent the % of T cells found in conjugates with APC. This is representative of 4 separate experiments. (B) Live cell imaging of immunological synapse formation by control and anergic T cells. Orange arrows indicate the T-APC interface where immune synapse is forming. Point of initial contact is defined as time 0 and mature immunological synapse is found in the right column at the indicated time point. At least 125 individual T-APC interactions were imaged for each T cell type over 5

separate experiments. (C). 3D imaging of fixed cells showing specific accumulation of MHC:peptide and TCR at the interface of control and anergic T cells and APC. (D) *en face* view to display the spatial distribution of accumulated MHC:peptide and TCR, which co-localize at the center of the T-APC interface for both control and anergic T cells. (E). Spatial distribution of ICAM-1 and GFP-tagged MHC:peptide at the T-APC interface. ICAM-1 forms a ring surrounding the central MHC:peptide. Images in C – E are representative of 5 separate experiments with more than 200 synapses imaged for both control and anergic T cells. Live cell images (B) collected with a 40× objective and fixed images (C–E) were collected with 60× objective. Size bar = 10μm.

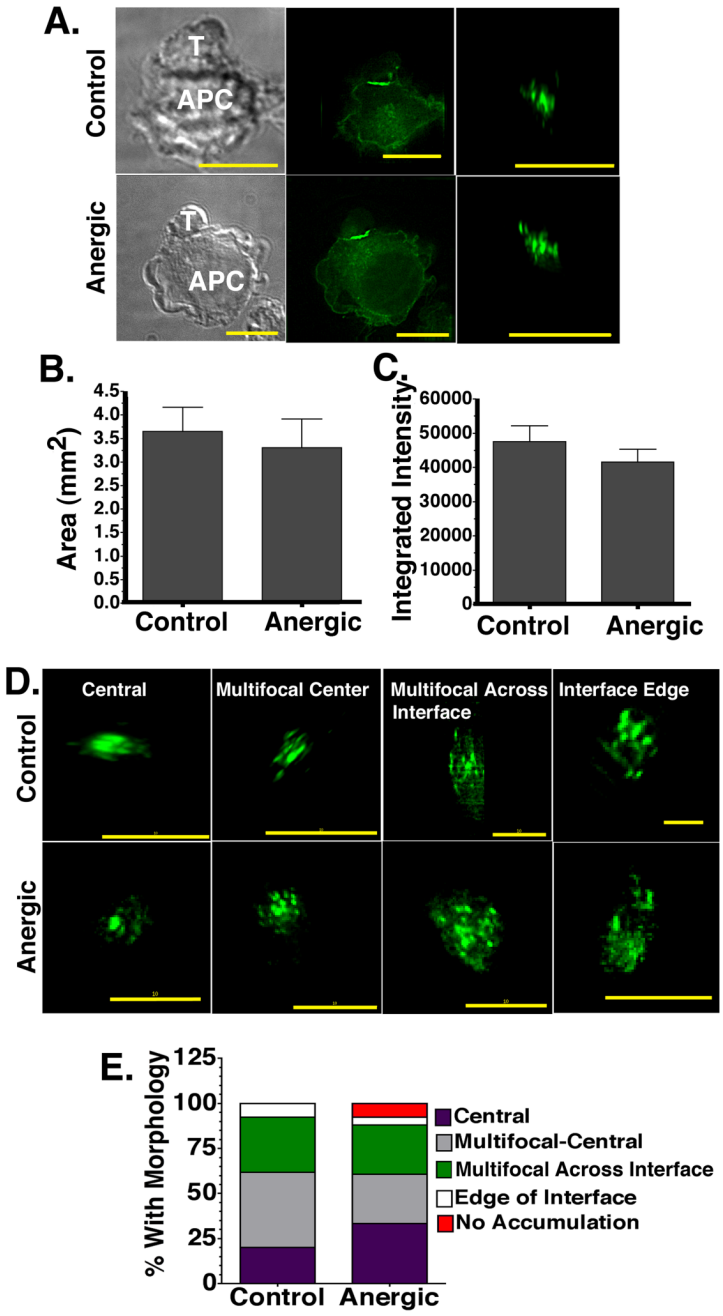

Figure 3. The amount, spatial distribution, and total area of accumulated MHC:peptide at the anergic immunological synapse is similar to control synapses

(A) DIC (left) and fluorescent images (center) of T-APC conjugates. The *en face* view of the T-APC interface is also shown (right). (B) The total area and (C) integrated intensity of accumulated MHC:peptide complexes ≥2 fold above background in *en face* views as in A. (D) Examples of MHC:peptide morphology at the T-APC interface for both control and anergic T cells. (E). Frequency of the distinct MHC:peptide accumulation morphologies identified in D. This is a single experiment representative of 7 separate experiments with more than 500 total control and anergic synapses imaged. There were 127 control synapses and 131 anergic

synapses in the experiment compared in E. All images were collected with 60× objective. Size bar = 10μm.

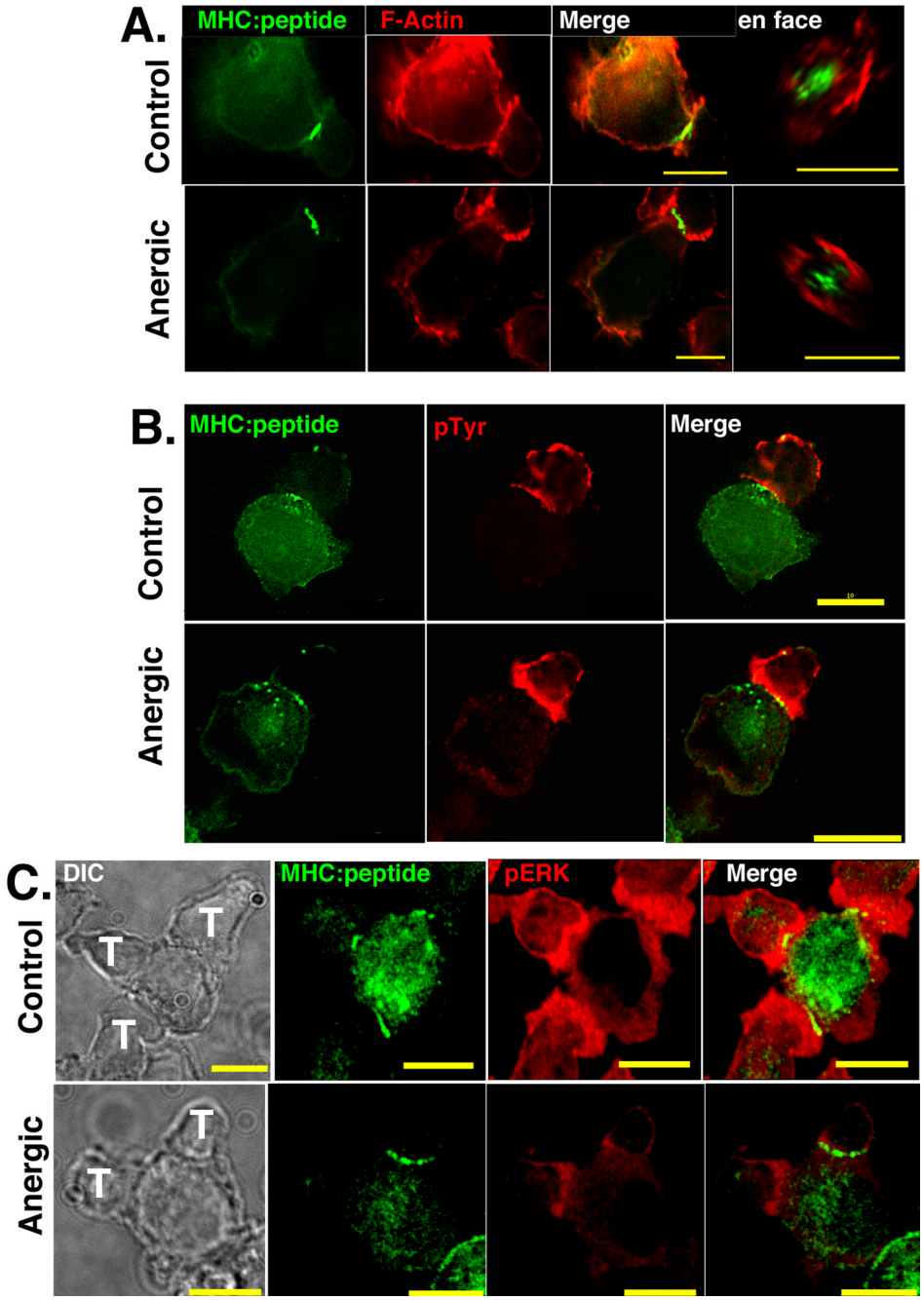

Figure 4. At the anergic synapse there is slightly increased accumulation of phosphorylated tyrosine residues, slightly reduced F-Actin accumulation, and significantly reduced phosphoERK 1/2

(A) Phalloidin staining showing slight reduction in the accumulation of F-actin to the anergic synapses. *en face* views (right) show that spatial distribution of accumulated F-actin is the same for control and anergic T cells. (B) Images of GFP-tagged MHC:peptide and phosphotyrosine at the T-APC interface of control and anergic T cells. Control cells have slightly less pTyr at the interface, but this difference is not significant. (C) Accumulation of phosphorylated ERK 1/2 is significantly reduced at the anergic synapse. Images in Fig. 4 are representative of 4 separate imaging experiments and more than 125 T-APC conjugates for each condition. There are two anergic cells associated with the APC in figure 4C whose immune synapses formed in

separate optical sections. The accumulation of GFP is similar in both, but because they are in separate optical planes, the GFP accumulation at both T-APC interfaces is not visible simultaneously in a single plane. Note that in Fig. 4, the intensity and brightness settings for each image in each panel are identical so perceived differences in brightness are representative of differences in staining intensity.

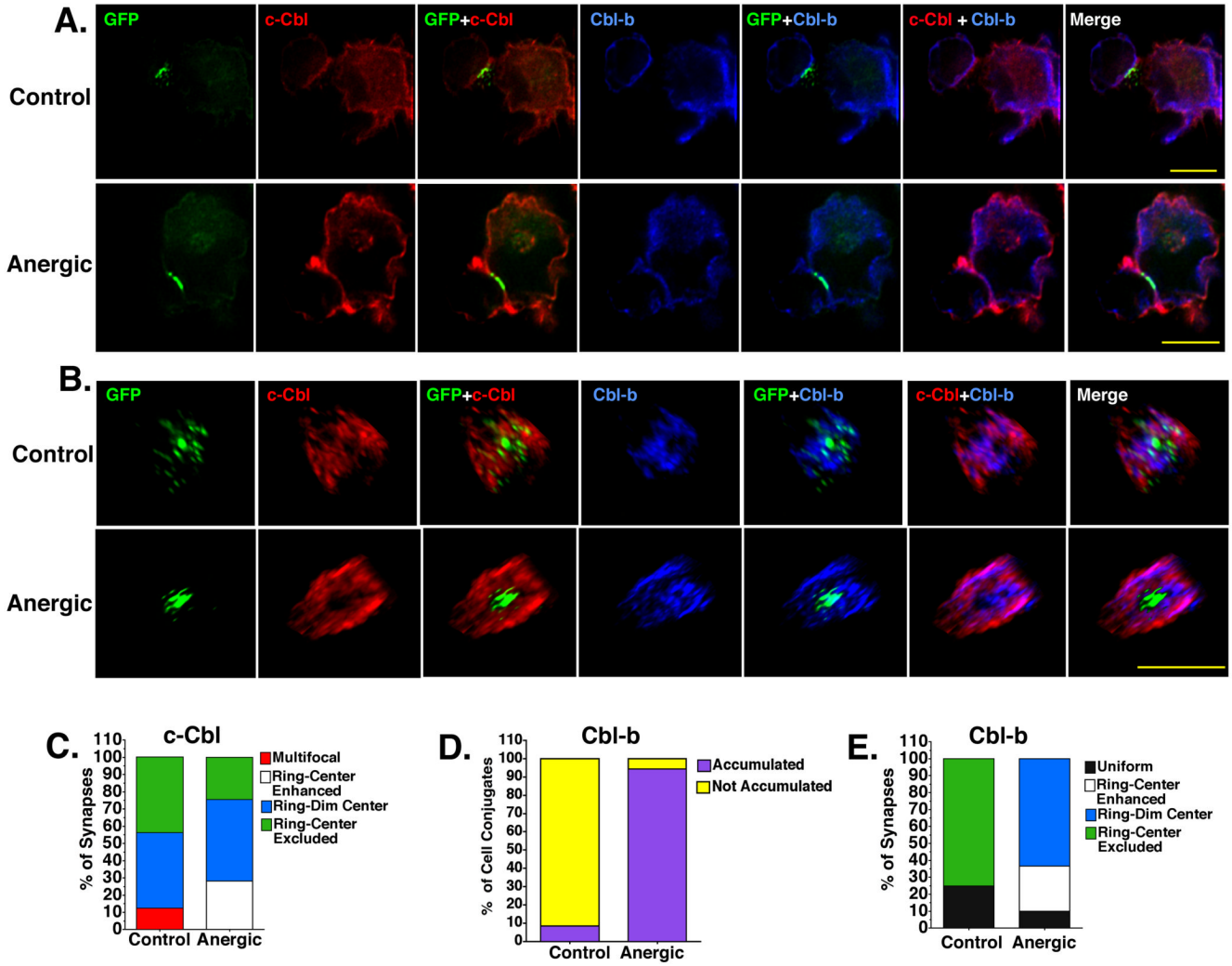

Figure 5. Cbl-b and c-Cbl are accumulated in the pSMAC of both control and anergic synapses and Cbl-b is also localized to the cSMAC in anergic cells only

(A) T-APC conjugates showing the accumulation of GFP-tagged MHC:peptide (green) c-Cbl (red) and Cbl-b (blue) at the T-APC interface. Intensity and brightness settings for each image in each panel are identical so perceived differences in brightness are representative of differences in staining intensity. (B) *En face* views of the synapses shown in A. Note: to allow visualization of all molecular species in the *en face* views, the intensity and contrast settings are NOT identical. Perceived differences in intensity do not reflect actual differences in staining intensity. Images are representative of 7 separate experiments and more than 500 images of both control and anergic cells. All images were collected with 60× objective. Size bar = 10μm. (C). The spatial distribution of c-Cbl at the control and anergic synapses. (D) The frequency of Cbl-b accumulation at the T-APC interface ≥2 fold above background for control and anergic cells. (E). Spatial distribution of Cbl-b is markedly different for control and anergic T cells.